

Establishment of a spontaneously transformed cell line (JU-PI) from a myxoinflammatory fibroblastic sarcoma

Tumor Biology
May 2018: 1–9

© The Author(s) 2018

Reprints and permissions:
sagepub.co.uk/journalsPermissions.nav
DOI: 10.1177/1010428318777936
journals.sagepub.com/home/tub

Klaus W Fagerstedt¹, Tarja Salonen², Fang Zhao¹, Soili Kytölä²,
Tom Böhling^{1,2} and Leif C Andersson¹ 

Abstract

Myxoinflammatory fibroblastic sarcoma is a soft-tissue neoplasm most frequently found in the distal extremities of middle-aged adults. Most myxoinflammatory fibroblastic sarcoma are low-grade tumors with propensity for local recurrence after incomplete removal. We report a myxoinflammatory fibroblastic sarcoma which developed in the foot of a 41-year-old male and showed an exceptionally aggressive course with metastatic spread and fatal outcome within 16 months. We managed to establish a spontaneously transformed continuous cell line, called JU-PI, from a metastatic lesion. The JU-PI cells have a sub-tetraploid karyotype including the 1;10 chromosomal translocation and amplification of the proximal end of 3p; these features are considered genetic signatures of myxoinflammatory fibroblastic sarcoma. Both the primary tumor and the JU-PI cells showed nuclear expression of the TFE3 transcription factor but TFE3-activating chromosomal rearrangements were not found. To our knowledge, JU-PI is the first established myxoinflammatory fibroblastic sarcoma cell line. JU-PI cells offer a tool for investigating the molecular oncology of myxoinflammatory fibroblastic sarcoma.

Keywords

Sarcoma cell line, myxoinflammatory fibroblastic sarcoma, TFE3, 3p11-3p12.1 amplification

Date received: 08 November 2017; accepted: 22 April 2018

Introduction

Myxoinflammatory fibroblastic sarcoma (MIFS) is a rare soft-tissue neoplasm that was described as a separate entity 20 years ago. MIFS most frequently arises as a painless slow-growing tumor in the distal extremities of adults in their 40s with no obvious gender predominance.^{1–3} The histology of MIFS may be pleomorphic, which makes initial diagnostics challenging. The tumor consists of spindle cells and epithelioid cells with abundant cytoplasm. Other tumor cells may have a vacuolated cytoplasm described as pseudolipoblasts. Also cells with large bizarre nuclei resembling Reed-Sternberg/Hodgkin's cells are frequently found.^{1,4–6} A common feature is the presence of areas of myxoid changes and infiltration of inflammatory cells including

lymphocytes, plasma cells, and macrophages in the tumor tissue.¹

MIFS is generally considered a neoplasm of low malignancy with propensity for local recurrence after incomplete removal.^{1,4} High-grade, metastasizing forms of MIFS are rare, reported to represent some 2% of the cases.³

Cytogenetic studies on MIFS have revealed a typical reciprocal translocation between chromosomes 1 and

¹Department of Pathology, University of Helsinki, Helsinki, Finland

²HUSLAB and Helsinki University Hospital, Helsinki, Finland

Corresponding author:

Leif C Andersson, Department of Pathology, University of Helsinki, PO Box 21 (Haartmaninkatu 3) 00014 Helsinki, Finland.

Email: Leif.Andersson@helsinki.fi



Creative Commons Non Commercial CC BY-NC: This article is distributed under the terms of the Creative Commons

Attribution-NonCommercial 4.0 License (<http://www.creativecommons.org/licenses/by-nc/4.0/>) which permits non-commercial

use, reproduction and distribution of the work without further permission provided the original work is attributed as specified on the SAGE and Open Access pages (<https://us.sagepub.com/en-us/nam/open-access-at-sage>).

10 t (1:10) (p22; q24), leading to juxtapositioning of parts of the TGFBR3 and MGEEA5 genes.^{7,8} No fusion product is formed, however, since the genes are transcribed in opposite directions. The translocation leads to secondary activation of the FGF8 gene that displays elevated expression in MIFS as in various neoplasms including synovial sarcoma and cancer of the breast and prostate.^{9,10} Another cytogenetic feature is amplification of the segment 3p11-3p12 leading to overexpression of the VGLL3 and CHMP2B genes.⁴ Amplification of VGLL3 is a frequent finding in different high-grade sarcomas.¹¹

No definite risk factors for MIFS have been identified. A role for repeated trauma has been suggested.¹² The presence of large “virocyte”-like tumor cells may indicate an infectious etiology, but consistent evidence for viral signatures has not been found.^{1,13}

Immortalized tumor cell lines offer tools for investigating the molecular biology of neoplasms. In this study, we describe the establishment and initial characterization of a spontaneously transformed continuous cell line, JU-PI from a metastatic MIFS. To the best of our knowledge, no MIFS-derived cell line has previously been reported.

Material and methods

Case presentation

A 41-year-old male came for surgical removal of a swelling on the dorsum of his foot. The first histopathological diagnosis was villonodular synovitis, a frequently encountered initial misdiagnosis of MIFS. Recurrence occurred within 6 months of the first meeting. IVADIC (Ifosfamide, vincristine, doxorubicin, dacarbazine)¹⁴ treatment was started during which the illness showed progression. Ten months after the initial surgery, a metastatic tumor was removed from the inguinal region. One month later, the patient returned

with metastatic lesions in the foot. Radiation therapy was initiated but the response was poor. Palliative amputation of the leg was performed after 1 month. New tumor growth occurred in the scar tissue. A whole-body CT scan revealed a widespread disease with metastases in both lungs and in the retroperitoneum. No response to treatment with etoposide was obtained and the patient succumbed to the tumor 16 months after the first intervention.

Tissue handling

Tissue samples were fixed in 10% phosphate buffered formalin and embedded in paraffin blocks for histology and immunohistochemistry. Fresh tissue was recovered from the recurrent tumor and the metastatic lesions, and was used for extraction of DNA and for in vitro culturing.

Immunohistochemistry

Immunohistochemistry on sections from formalin-fixed and paraffin embedded material was performed using a Ventana Benchmark XT automated stainer (Ventana Medical Systems, Inc., USA). The primary antibodies employed are listed in Table 1. Cells were cultivated on object glasses (SuperFrost Ultra Plus®, Menzel GmbH & Co KG, Saarbrückener Str. 248, D-38116 Braunschweig), and fixed for 30 min in 10% formalin for immunocytochemistry.

Establishment of a cell line

Fresh metastatic tumor tissue recovered from the groin was minced with a scalpel. The tissue fragments were treated with collagenase (2 mg/mL, Type IV, Sigma) and DNAse (100 µg/mL, Sigma) in serum-free culture medium for 4 h at 37°C under agitation. The cell suspension was pelleted by centrifugation, washed once

Table 1. Antibodies used for immunohistochemistry.

Antigen	Clone	Dilution	Manufacturer
Vimentin	V9	1:500	Dako, M0725
CAM5.2	CAM5.2	1:50:00	BD, 345779
S-100	Polyclonal	1:700	Dako, Z0311
HMB-45	HMB45	1:100	Dako, M0634
Smooth muscle actin	1A4	1:100	Dako, M0851
CD3	PS1	1:100	Novocastra, NCL-cd3-PS1
CD20	L26	1:1000	Dako, M0755
CD31	JC70A	1:25	Dako, M0823
CD34	My10+8G12	1:50	BD, 347660
CD56	504	1:50	Novocastra, NCL-CD56-504
CD68	KPI	1:400	Dako, M0814
Ki-67	MIB-1	1:75	Dako, A0047
TFE3	MRQ-37	RTU	Roche/Ventana, 760-4622

with RPMI-1640 culture medium, plated in RMPI-1640 culture medium supplemented with 10% fetal bovine serum and antibiotics (Penicillin and Streptomycin) and cultured at 37°C in a humidified atmosphere of 5% CO₂ in air. Focal outgrowth of adherent, spindle-shaped cells was seen within 1 week of primary culturing. After an initial phase of slow growth for about 1 month, a more rapidly proliferating monomorphic population of spindle shaped cells emerged. The cultures were divided twice weekly after detachment of the cells by treatment with Trypsin-Versene (© 2009 Lonza Walkersville, Inc.). We called the established cell line JU-PI. The cell line (passage 9) was cryopreserved from 2001 until 2016 when this study was initiated.

Isolation of DNA

DNA was isolated using a proteinase K-based method according to the manufacturer's instructions (Thermo Fisher Scientific Baltics UAB, V.A. Graiciuno 8, LT-02241 Vilnius, Lithuania). The isolated JU-PI DNA was from a passage 36.

Microsatellite analysis

Microsatellite analysis of DNA isolated from fresh frozen tumor tissue and JU-PI cells (passage 36) was performed by polymerase chain reaction (PCR) amplification of 11 microsatellite loci using fluorescently labeled primers. The PCR products were separated by capillary electrophoresis (3130XL Genetic Analyzer, Applied Biosystems) and analyzed by using GeneMapper 5 software.

Comparative genomic hybridization

Comparative genomic hybridization (CGH) with DNA from fresh tumor tissue and JU-PI cells (passage 36) was carried out using Cancer + SNP 4 × 180k microarray (Oxford Gene Technology, Oxford, UK). Labelling, hybridization, scanning, and analysis were done according to the manufacturer's instruction. The microarray slides were scanned using an Agilent DNA Microarray Scanner G2505 (Agilent Technologies Inc, Santa Clara, CA, USA) and filtered with Feature Extraction software v12.0.07 (Agilent Technologies). The Cytosure Software v4.9 (Gh19) (Oxford Gene Technology) was used for graphic analysis of the data.

Karyotype and multicolor FISH

Cell culturing and metaphase-fluorescence in situ hybridization (FISH) preparations were done according to standard cytogenetic procedure.¹⁵ Twenty-four color FISH karyotyping was performed with 24XCyte mFISH probe kit (MetaSystems GmbH, Altlussheim, Germany). Hybridizations and post-hybridization washes were

performed according to the manufacturers' instructions. (A Zeiss Axioplan 2 Microscope equipped with specific filters was used.) Images were captured and processed using the Isis/Multicolor FISH imaging system (MetaSystems).

Electron microscopy

Cells in culture were fixed by pre-warmed 2.5% glutaraldehyde in culture medium at 37°C for 15 min, scraped off the plates and pelleted by centrifugation. The pellets were further fixed in 2.5% glutaraldehyde for 1 h. The fixed sample was post-fixed by 1% osmium tetroxide, dehydrated in graded ethanol, embedded by Epoxy LX-112 resin. Sections of 60–80 nm thickness were cut, observed under a JEOL JEM1400 (Tokyo, Japan) at 80 kV. Digital electron micrographs were taken by a Morada TEM digital camera (EMSIS GmbH, Muenster, Germany).

Growth curve

The cell numbers in triplicate daily samples from parallel JU-PI cultures were counted in a hemocytometer.

Results

Morphology of the primary and recurrent tumors

Myxoid and solid areas could be seen in both the primary and metastatic tumors, with more abundant solid areas in the metastases. Some slit-like spaces without any lining cells as well as necrotic areas were found. The tumor cells were epithelioid or spindle shaped with large nucleoli, and their mitotic activity was high. Atypical mitotic figures were observed in both the primary and metastatic tumors. Occasional multinucleated giant cells with atypical nuclei were seen (Figure 1(a) and (b)). Inflammatory cells accumulated mostly around necrotic areas but also lining fibrotic streaks in the tumor. In some of the tumor cells, intracytoplasmic accumulation of period acid-Schiff (PAS) material was observed (Figure 1(c) and (d)).

Immunohistochemistry

Immunohistochemistry performed on sections from both the primary and metastatic tumors showed positivity for vimentin and TFE3. The TFE3 staining was nuclear in the tumor cells (Figure 1(e) and (f)). The proliferation index measured by Ki-67 was 10% in the primary tumor and over four times higher in the metastases (Figure 1(g) and (h)). The other antibodies listed in Table 1 yielded no positive staining of the tumor cells.

Genetics of the tumor

CGHs were performed using tumor-derived DNA in 2000–2001. The main findings were loss of chromosome

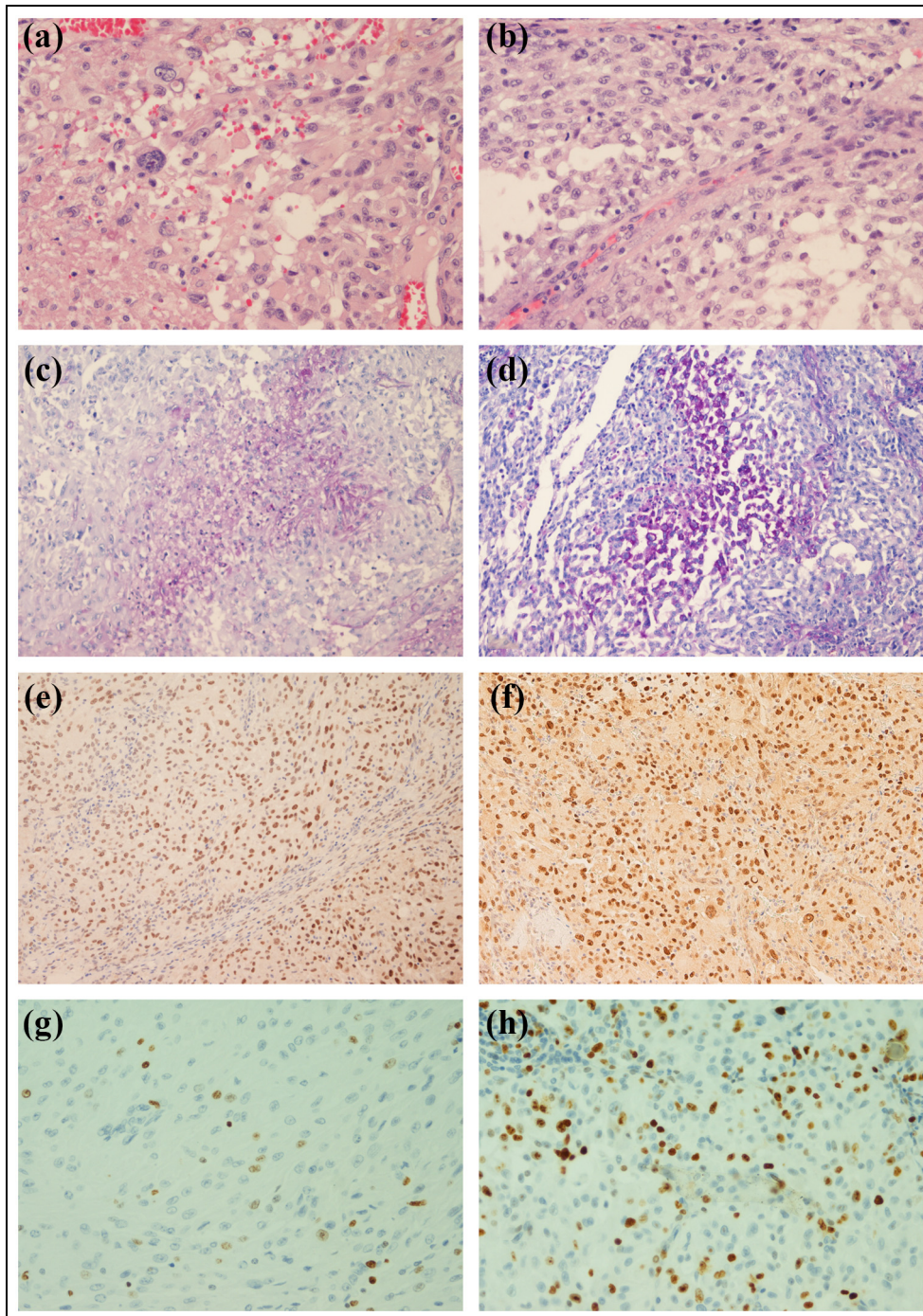


Figure 1. Histology and IHC of the primary tumor (a, c, e, g) and of the metastatic tumor (b, d, f, h). PAS-positive material in the tumor cells (c, d). Nuclear localization of TFE expression (e, f) and of Ki-67 expression (g, h).

13 and amplification of p12.3 close to the centromere on chromosome 3.

Growth pattern of JU-PI cells

After plating, spindle-shaped JU-PI cells grew in adherent monolayers. Before reaching confluence, the cells

piled up in loose, organoid-like aggregates. Most cells contained a single nucleus with one or several more prominent nucleoli. Accumulation of intracytoplasmic light-refracting granules of 0.5–1 μm was seen after extended cultivation, particularly in cells forming adherent aggregates (Figure 2(a)). Phase contrast microscopy revealed an abundance of slender thread-

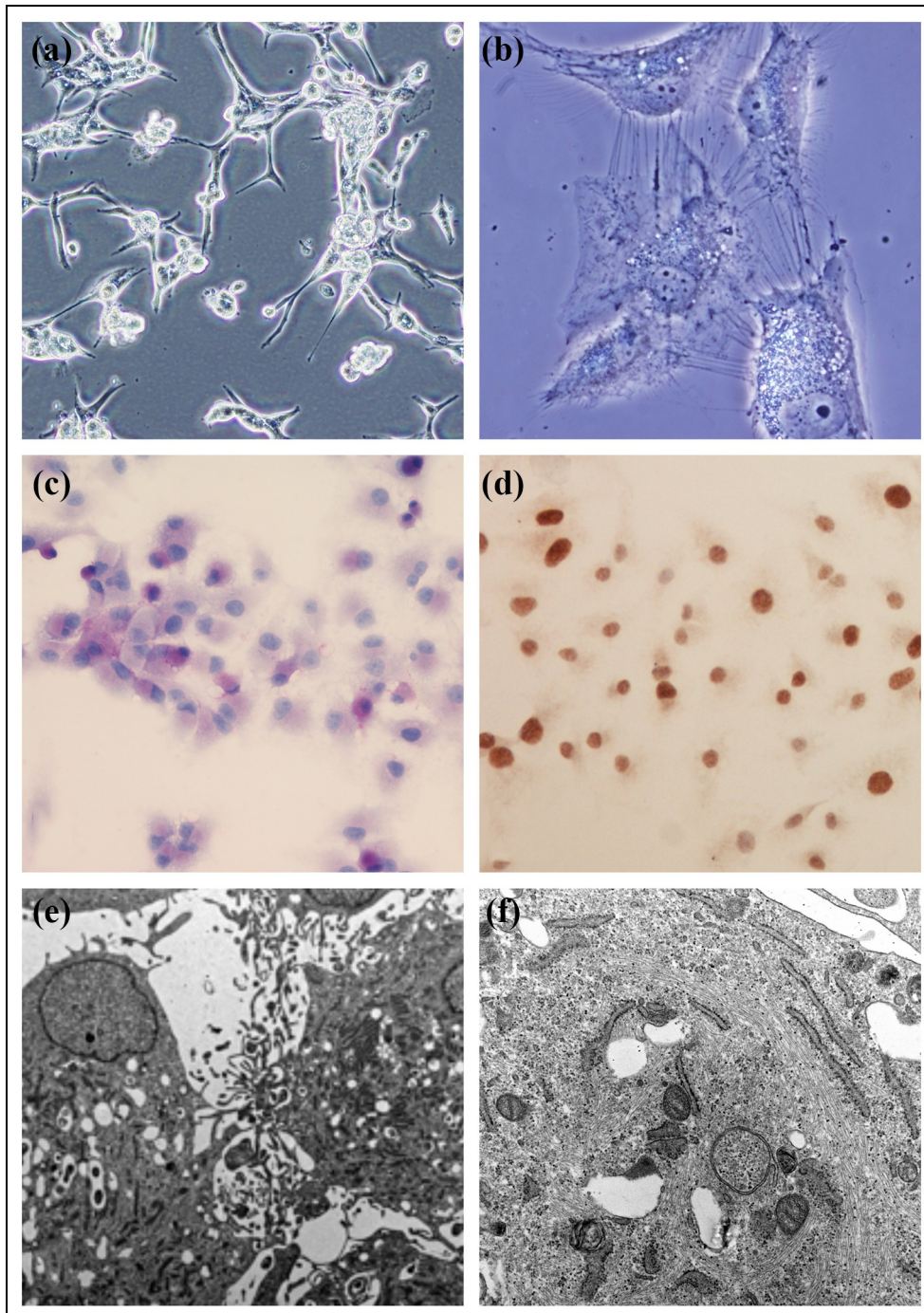


Figure 2. Morphology and immunocytochemistry of JU-PI cells. Phase-contrast pictures of growing cells (100 \times) (a) and at higher magnification (400 \times) (b) showing intracytoplasmic light-refracting material and slender membrane protrusions. Intracytoplasmic PAS-positive material (c) and nuclear expression of TFE3 (d). TEM pictures of JU-PI cells (e, f).

like protrusions on the cell surface membranes (Figure 2(b)).

Growth curve

The growth curve revealed proliferation for 4 days after which a plateau was reached. The doubling time was calculated to be 1.1 days (Figure 3).

Staining of the JU-PI cells

The staining of JU-PI cells cultivated on object glasses showed intracytoplasmic accumulation of PAS-positive material in many cells (Figure 2(c)). Immunocytochemistry revealed nuclear positivity for TFE3 (Figure 2(d)).

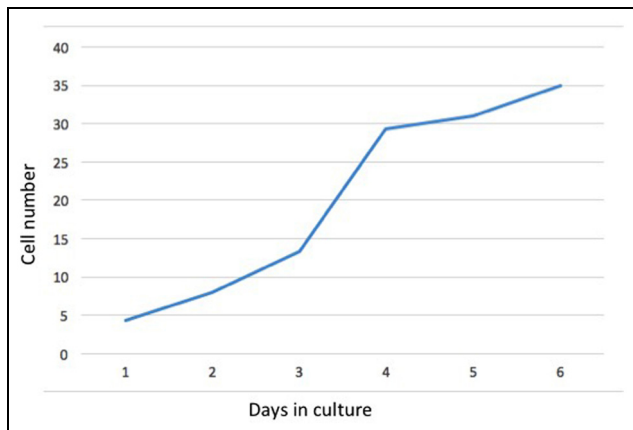


Figure 3. Growth curve of JU-PI cells.

TEM

TEM images showed abundant 10 nm intermediate filaments organized in a random fashion. Aggregation of filaments to fibrils of 30–40 nm in diameter was also seen. Some fibrils appeared densely packed in one pole displacing the organelles to the other side of the cell. The filaments were not arranged in crystal-like aggregates like those described in alveolar soft part sarcoma. In some cells, the RER was found to contain proteinaceous masses. An abundance of dendrite-like projections on the cell surface membrane was also evident. No intercellular junctions were formed even when the cells were closely positioned with juxtaposed cell membranes (Figure 2(e) and (f)).

Genetics of the cell line

The results of the chromosome painting (M-FISH) done on JU-PI revealed a nearly tetraploid chaotic karyotype with chromosome numbers ranging between 81 and 97. A consistent finding was the loss of chromosomes 13 and Y (Figure 4c).

The most frequently found translocations were t(1;5), t(1;10), t(7;13), t(1;15), and t(14;17). CGH, using JU-PI cell DNA showed a prominent amplicon in the chromosomal region 3p11-3p12.3 (Figure 4(b)). CGH also confirmed the loss of genetic material of whole chromosomes Y and 13. The findings on chromosomal level are summarized in Figure 4(a). The lack of chromosome 13 implies absence of the tumor suppressor gene RB1. The loss of 17p13.1 containing the TP53 gene was also revealed by CGH. In addition, several deletions or amplifications of chromosomal regions containing genes of importance for neoplastic growth were found. These are summarized in Table 2.

To confirm the derivation of the JU-PI cell line from the original tumor, we performed a microsatellite analysis of 11 microsatellite loci. They showed identical

Table 2. Chromosomal aberrations revealed by CGH with JU-PI cell DNA.

	Gene(s) involved	Found in neoplasm/function
Losses		
1p21.1	AMY2A	Gastric cancer
10q25.1-q26.3	NEURL1	Enhancement of apoptosis
15q11.2-q22.2	?	Aggressiveness of urothelial cancer
17p13	p53	Many cancers
21q22	?	Uterine leiomyosarcoma
22q11	SMARCB1	Malignant rhabdoid tumor
Gains		
14q11	BCL2L2	Osteosarcoma

results in the tumor and the cell line, which demonstrates that the cell line JU-PI originates from the resected tumor material (data not shown). The findings also confirmed the CGH results showing deletions of genetic material from chromosome 13 and loss of the whole Y chromosome.

Discussion

We report the establishment of a spontaneously transformed continuous cell line from a metastatic lesion of an exceptionally aggressive MIFS with early metastatic spread and fatal outcome.

MIFS usually displays a benign clinical course. Laskin et al.¹⁶ reported 104 cases of MIFS, and of 59 cases with accessible follow-up, only one presented with metastatic disease. Michal et al.⁶ collected 23 cases of high-grade MIFS out of which 9 developed a metastatic disease which became fatal for 7 patients.

The primary tumor described here was initially (in 2000) diagnosed as proliferative villonodular synovitis. Later biopsies from the metastases were diagnosed as sarcoma NOS. Immunohistochemistry did not show staining patterns of differential diagnostic value. After establishment of the cell line, the morphology of the primary tumor and the metastatic lesions were re-evaluated and found to fulfill the histological criteria described for MIFS. TEM also revealed ultrastructures typical to sarcoma and divergent from TEM findings in carcinoma.

The JU-PI cell line was considered established to be already after 6 weeks of culture. The growth pattern of adherent spindle shaped cells is typical for mesenchymal neoplasms. Piling up of cells in organoid-like aggregates occurs before the culture reaches confluence. These cell aggregates did not display invasive growth in semisolid medium (Matrigel) (data not shown). Whether the JU-PI cells are tumorigenic upon heterotransplantation remains to be established. The accumulation of slightly

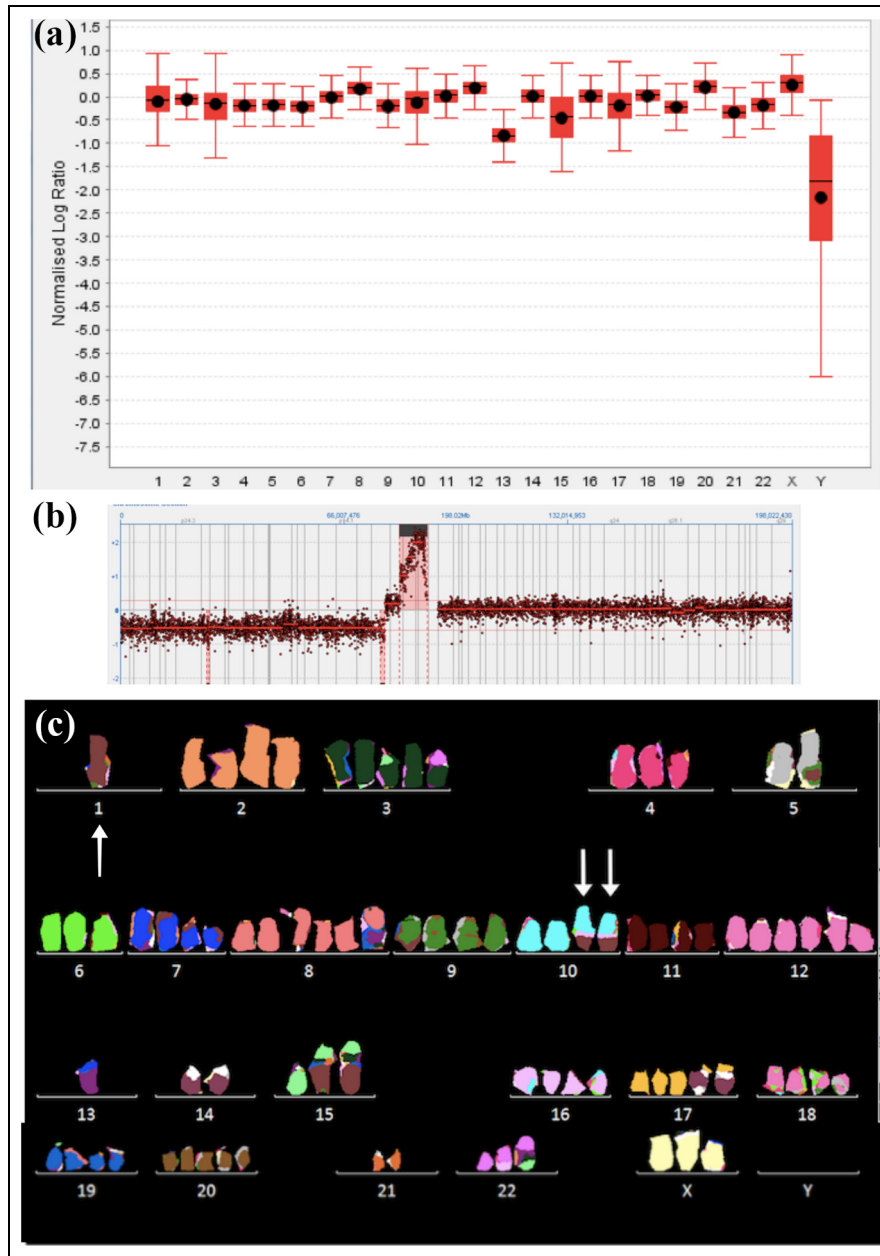


Figure 4. Summary of the CGH on all chromosomes showing loss of the Y chromosome and chromosome 13 (a). CGH profile showing the prominent amplicon on chromosome 3 (3p11-3p12.2) (b). Multicolor FISH of JU-PI karyotype showing the t(1;10) translocation (arrows) and lack of Y chromosome (c).

light-refracting cytoplasmic granules prompted us to use TEM to investigate the JU-PI cells. The granular material, however, did not appear as the rhomboid crystals typically found in alveolar soft part sarcoma but rather as proteinaceous aggregates without a clear structure. The composition of these granules is a matter for forthcoming investigations.

The primary tumor as well as the metastases showed areas of diastase-resistant PAS-positive staining both in the tumor cells and the stroma. Intracytoplasmic accumulation of PAS-positive material was also seen in the

JU-PI cells. This most likely represents mucopolysaccharides that are compatible with the myxoid changes characteristic for MIFS. Additional biochemical studies are nevertheless required to disclose the molecular nature of the PAS-positive material.

We found nuclear expression of TFE3 both in the primary tumor and in JU-PI cells. We did not find previous reports on the expression of TFE3 in high-grade variants of MIFS which may be due to the relative rarity of the tumor. TFE3 is a transcription factor involved in SMAD2/3 nuclear signaling and TGF- β signaling

pathways. Dysregulated TFE3 expression occurring particularly via gene fusions has been found to display oncogenic activity. TFE3 expression is considered to be a marker for alveolar soft part sarcoma where its expression results from a translocation (X:17) (p11:q25) that gives rise to ASPSCR1-TFE3 fusion transcripts. Additional fusion partners of TFE3 (PRCC, SFPQ, NONO, CLTC, and YAP1^{17–20}) have been identified in renal cell cancer and perivascular epithelioid cell tumors (PEcomas).

Karyotype analysis was not done on the primary tumor material. In the JU-PI cell line, we did not find known TFE3-activating chromosomal rearrangements. We also performed RT-PCR investigation on mRNA isolated from JU-PI cells but could not find evidence for expression of either type 1 or type 2 ASPSCR1-TFE3 fusion transcripts (data not shown). Elevated expression of TFE3 has been reported to occur in hepatic angioleiomyoma also in the absence of known genetic rearrangements. It remains to be investigated whether genetic rearrangements in JU-PI cells are driving the TFE3 expression or whether it is caused by a gene dose effect due to chromosome X polysomy.

A recurrent t(1;10) translocation that is a genetic signature of MIFS⁸ was found in the karyotypes of JU-PI cells. The same chromosomal rearrangement occurs also in hemosiderotic fibrolipomatous tumors. This has triggered speculations about the interrelationship between these two rare soft-tissue neoplasms. This question was recently thoroughly addressed by Boland and Folpe²¹ in a comprehensive review which came to the conclusion that MIFS and hemosiderotic fibrolipomatous tumor apparently represent different entities.

CGH using DNA from the primary tumor and JU-PI cells revealed amplification of the proximal end 3p (3p11-3p12.3). This change, in addition to MIFS has been observed in a variety of high-grade sarcomas. This amplicon has been shown to induce overexpression of the VGLL3 and CHMP2B genes. Elevated expression levels of VGLL3, which acts as a cofactor of the TEAD family of transcription factors have been found to stimulate tumor cell migration and invasion.⁴

Despite the male origin of the tumor, the Y chromosome was missing from all the analyzed karyotype spreads of JU-PI cells. Deletion of the Y chromosome has been reported to occur in a variety of neoplasms such as prostate cancer, pancreatic cancer, squamous cell carcinoma of the head and neck, leukemia, hepatocellular carcinoma, malignant peripheral nerve sheath tumor angiosarcoma, and Kaposi's sarcoma.^{22–24}

In summary, we describe a high-grade, rapidly fatal case of MIFS from which we managed to establish a spontaneously transformed cell line JU-PI. The JU-PI cells offer a novel model for studying the molecular tumor biology of MIFS and related soft-tissue

neoplasms. The JU-PI cell line is freely available for interested investigators.

Acknowledgements

The authors thank Dr. Markku Miettinen for expert reviewing of the histology of the primary tumor. Ms. Tiiu Arumäe is acknowledged for excellent technical assistance.


Declaration of conflicting interests

The author(s) declared no potential conflicts of interest with respect to the research, authorship, and/or publication of this article.

Funding

The author(s) disclosed receipt of the following financial support for the research, authorship, and/or publication of this article: The study was supported by The Academy of Finland, The Sigrid Jusélius Foundation, The Magnus Ehrnrooth Foundation, Finska Läkaresällskapet, and Livoch Hälsa.

ORCID iDs

Leif C Andersson  <https://orcid.org/0000-0001-6264-9620>

References

1. World Health Organization Classification of Tumors. Myxoinflammatory fibroblastic sarcoma. In: Christopher DM, Fletcher K and Krishnan UFM (eds) *Pathology and genetics of tumors of soft tissue and bone*. 1st ed. Lyon: IARC Press International Agency for Research on Cancer (IARC), pp. 96–97, 2002.
2. Kato M, Tanaka T and Ohno T. Myxoinflammatory fibroblastic sarcoma: a radio graphical, pathological, and immunohistochemical report of rare malignancy. *Case Rep Orthop*. Epub ahead of print 18 May 2015. DOI: 10.1155/2015/620923.
3. Lombardi R, Jovine E, Zanini N, et al. A case of lung metastasis in myxoinflammatory fibroblastic sarcoma: analytical review of one hundred and thirty eight cases. *Int Orthop* 2013; 37(12): 2429–2436.
4. Hallor KH, Sciot R, Staaf J, et al. Two genetic pathways, t(1;10) and amplification of 3p11–12, in myxoinflammatory fibroblastic sarcoma, haemosiderotic fibrolipomatous tumour, and morphologically similar lesions. *J Pathol* 2009; 217(5):716–727.
5. Sakaki M, Hirokawa M, Wakatsuki S, et al. Acral myxoinflammatory fibroblastic sarcoma: a report of five cases and review of the literature. *Virchows Arch* 2003; 442(1):25–30.
6. Michal M, Kazakov DV, Hadravsky L, et al. High-grade myxoinflammatory fibroblastic sarcoma: a report of 23 cases. *Ann Diagn Pathol* 2015; 19(3):157–163.
7. Antonescu CR, Zhang L, Nielsen GP, et al. Consistent t(1;10) with rearrangements of TGFBR3 and MGEA5 in both myxoinflammatory fibroblastic sarcoma and hemosiderotic fibrolipomatous tumor. *Gene Chromosome Canc* 2011; 50(10):757–764.

8. Mertens F, Panagopoulos I and Mandahl N. Genomic characteristics of soft tissue sarcomas. *Virchows Arch* 2010; 456(2):129–139.
9. Nishio J, Iwasaki H, Nabeshima K, et al. Cytogenetics and molecular genetics of myxoid soft-tissue sarcomas. *Genet Res Int*. Epub ahead of print 21 March 2011. DOI: 10.4061/2011/497148.
10. Liu R, Huang S, Lei Y, et al. FGF8 promotes colorectal cancer growth and metastasis by activating YAP1. *Oncotarget* 2014; 6(2):935–952.
11. Helias-Rodzewicz Z, Perot G, Chibon F, et al. YAP1 and VGLL3, encoding two cofactors of TEAD transcription factors, are amplified and over expressed in a subset of soft tissue sarcomas. *Gene Chromosome Canc* 2010; 49(12):1161–1171.
12. Marusic Z, Cengic T, Dzombeta T, et al. Hybrid myxoinflammatory fibroblastic sarcoma/hemosiderotic fibrolipomatous tumor of the ankle following repeated trauma. *Pathol Int* 2014; 64(4):195–197.
13. Meis-Kindblom JM and Kindblom LG. Acral myxoinflammatory fibroblastic sarcoma: a low-grade tumor of the hands and feet. *Am J Surg Pathol* 1998; 22(8): 911–924.
14. Wiklund TA, Blomqvist CP, Virolainen M, et al. Ifosfamide, vincristine, doxorubicin and dacarbazine in adult patients with advanced soft-tissue sarcoma. *Cancer Chemotherapy Pharmacol* 1992; 30(2):100–104.
15. Howe B, Umrigar A and Tsien F. Chromosome preparation from cultured cells. *J Vis Exp* Epub ahead of print 28 January 2014. DOI: 10.3791/50203.
16. Laskin WB, Fetsch JF and Miettinen M. Myxoinflammatory fibroblastic sarcoma: a clinicopathologic analysis of 104 cases, with emphasis on predictors of outcome. *Am J Surg Pathol* 2014; 38(1):1–12.
17. Argani P, Antonescu CR, Couturier J, et al. PRCC-TFE3 renal carcinomas: morphologic, immunohistochemical, ultrastructural, and molecular analysis of an entity associated with the t(X;1)(p11.2; q21). *Am J Surg Pathol* 2002; 26(12):1553–1566.
18. Rao Q, Shen Q, Xia QY, et al. PSF/SFPQ is a very common gene fusion partner in TFE3 rearrangement-associated perivascular epithelioid cell tumors (PEComas) and melanotic Xp11 translocation renal cancers: clinicopathologic, immunohistochemical, and molecular characteristics suggesting classification as a distinct entity. *Am J Surg Pathol* 2015; 39(9):1181–1196.
19. Xia QY, Wang Z, Chen N, et al. Xp11.2 translocation renal cell carcinoma with NONO-TFE3 gene fusion: morphology, prognosis, and potential pitfall in detecting TFE3 gene rearrangement. *Mod Pathol* 2017; 30(3): 416–426.
20. Antonescu CR, Le Loarer F, Mosquera JM, et al. Novel YAP1-TFE3 fusion defines a distinct subset of epithelioid hemangioendothelioma. *Gene Chromosome Canc* 2013; 52(8):775–784.
21. Boland JM and Folpe AL. Hemosiderotic fibrolipomatous tumor, pleomorphic hyalinizing angiectatic tumor, and myxoinflammatory fibroblastic sarcoma: related or not? *Adv Anat Pathol* 2017; 24: 268–277.
22. Pyakurel P, Montag U, Castanos-Velez E, et al. CGH of microdissected Kaposi's sarcoma lesions reveals recurrent loss of chromosome Y in early and additional chromosomal changes in late tumour stages. *AIDS* 2006; 20(14): 1805–1812.
23. Noveski P, Madjunkova S, Sukarova Stefanovska E, et al. Loss of Y chromosome in peripheral blood of colorectal and prostate cancer patients. *PLoS ONE* 2016; 11(1): e0146264.
24. Mandahl N, Jin YS, Heim S, et al. Trisomy 5 and loss of the Y chromosome as the sole cytogenetic anomalies in a cavernous hemangioma/angiosarcoma. *Gene Chromosome Canc* 1990;1(4):315–316.